

Highly Porous ZnO Nanoparticles for LPG Gas Sensor

B. M. Sargar

Material Research Laboratory, Department of Chemistry, Jaysingpur College, Jaysingpur, Kolhapur (M.S), India - 416101

Abstract: Zinc oxide proves its usefulness in diverse fields. It can be synthesized by different physical as well as chemical methods. In present work, Zinc oxide (ZnO) powder was prepared successfully by chemical combustion method. The prepared powder were analysed by various instrumental techniques. The structural property was studied by using X-ray diffraction study. It is showed that ZnO exhibit hexagonal wurtzite structure with crystalline size of 22.77 nm. SEM reveals that morphology of the synthesized powder exhibit porous structure. The elemental composition was confirmed by EDAX analysis. Optical study showed that the band gap of synthesized ZnO is 3.2eV and it is in good agreement with reported value. Finally, Gas response characteristic of ZnO were systematically studied for LPG at different operating temperatures and at different concentrations. ZnO shows maximum response of 54.3% at temperature 300°C for 10ppm LPG gas concentration.

Keywords: Combustion method, ZnO, Gas sensing

1. Introduction

Semiconducting metal oxides viz. SnO₂, CuO, ZnO, TiO₂ and Fe₂O₃ finds promising roles in detection and monitoring of hazardous gases. Among all them Zinc oxide is versatile semiconducting material which is extensively used for detection of gases NH₃, CO, CH₄[1]. ZnO is n-type material having band gap 3.2eV at room temperature and binding energy 60eV [2-3]. Today, gas sensor is very much essential for detection of toxic, flammable, hazardous and combustible gases which causes air pollution as well as accidents [4]. A Singh et.al [5], Nicolaebarsan et.al [6] and Wen An [7] had reported commonly accepted mechanism of gas sensor. In n-type semiconductor adsorption of oxygen at the surface which involves trapping of electron from the semiconductor that results in decrease of conductance. In the presence of reducing gases like LPG, NH₃, H₂S, H₂ etc. the reaction of test gas with adsorbed oxygen returns the electrons to the semiconductor which results into increase in conductance but this reaction reversed in presence of oxidizing gases like Cl₂, NO₂ etc.

Zinc oxide synthesized by numerous methods like Hydrothermal [8-9], Sol-gel [10], Chemical bath deposition (CBD) [11], Successive ionic layer adsorption and reaction (SILAR) [12], Spray Pyrolysis [13] etc. depending on the various reaction condition various morphologies have been reported viz. Nano belts [14-15], nanowires [16-17], Nano flowers [18] and nanorods [19] etc. ZnO is extensively studied for their optical, structural, morphological and electrical properties for various applications [20-22]. ZnO is also useful material for the detection of various reducing gases like LPG [23], Hydrogen and Ethanol [24]. So, in this work LPG gas sensing behavior of combustion method synthesized ZnO has been reported.

2. Experimental

Precursors utilized for the synthesis of ZnO are Zinc Nitrate [Zn(NO₃)₂], Glycine [C₂H₅NO₂] were used as source of Zinc and fuel respectively. All chemicals were purchased by Thomas Baker and used without any purification.

ZnO was synthesized by a chemical combustion method. A solutions of 0.3 N Zn(NO₃)₂ was mixed with 0.3N glycine solution which acts as fuel. The mixed solution was taken in a large crystallizing dish and kept over a hot plate for auto combustion at 473 K. After the complete evaporation of water, a reddish black colored thick gel was formed, which was ignited and it was resulted into brown colored Zinc oxide. The synthesized powdered sample was annealed for 2 hours at temperature 673K. Then prepared sample was characterized by powder X-ray diffraction (XRD), Scanning electron Microscopy (SEM), Energy Dispersive X Ray Analysis (EDAX) then after samples were applied for gas sensing measurement.

The LPG sensing properties of ZnO films were studied using a "static gas -sensing system." There were electrical feeds through the base plate. The heater was fixed below the base plate to heat the sample under test up to desired operating temperatures. Al-Cr thermocouple was used to sense the operating temperature of the sensors. The output of the thermocouple was connected to digital temperature indicators. A gas inlet valve was provided at one port of the base plate. The required gas concentration inside the static system was attained by injecting a known volume of test gas using a gas-injecting syringe. For electrical measurements, paste contacts were made on the ZnO sample of area 1 cm×1 cm. the silver contacts showed ohmic behavior. With this instrumental arrangement gas response for ZnO was measured.

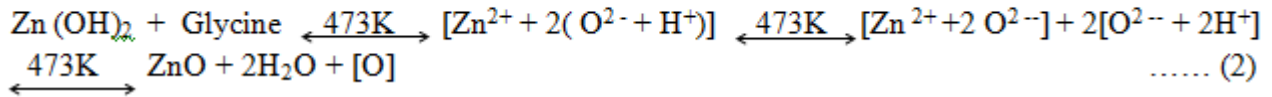
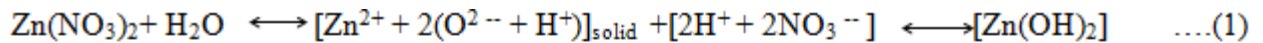
3. Results and Discussion

3.1 Synthesis Mechanism

Nanoparticles growth involves two steps. In first step, dissociation of nitrate salt of Zinc takes place in distilled water. Appropriate concentrated solution of zinc nitrate has been prepared in distilled water with continuous stirring. After 5 min, stirred solutions were converted in to water soluble hydroxides of Zinc. This reaction can be represented by following reaction mechanism (1).

In second step, above hydroxide solutions of Zinc was mixed with the glycine which acts as fuel and heated over a hot plate at temperature 473K. After 2 hours wine red coloured sol has been formed. Water vapours released during complete combustion of reaction mixture. Finally,

Continuous heating of sol get ignited which resulted into pale brown coloured Zinc oxide nanoparticles. Nanoparticles so obtained were further subjected to annealing to remove hydrated water contain and further growth of nanoparticle (2).



3.2 Structural Analysis

The powder X Ray Diffraction patterns of ZnO shown in Figure 1. Synthesized sample was characterized by Philips automated X-Ray diffractometer (PW-3710) equipped with crystal monochromator employing Cu-K α radiation of wavelength 1.5406 Å in 2 θ range 15°- 80°. The XRD pattern shows hexagonal wurtzite crystal structure of ZnO. No reflections due to any secondary phase are detected in the XRD pattern. The peaks are observed at 2 θ values of 31.81°, 34.54°, 36.29°, 47.53°, 56.58°, 62.85° and 67.92° are corresponding to (100), (002), (101), (102), (110), (103), (112). The obtained XRD spectra was confirmed by matching with the JCPDS file [No. 36-1451] [19]. The average particle sizes were calculated from X-ray line broadening using the Scherer formula (1). The average crystalline size calculated for ZnO is 22.77 nm.

$$D = \frac{K\lambda}{\beta \cos \theta} \quad \dots\dots(1)$$

Where, K is constant called as the shape factor = 0.94, λ is the Wavelength, β is Full width at half maximum (FWHM) given in radian, θ = It is the Bragg's angle, D = Nanoparticle size in nanometer.

3.3 SEM and EDAX

Surface morphological study of ZnO was carried out by scanning electron microscopy (SEM). Figure 2 (a-c) shows SEM micrographs at different magnifications. SEM depicts interconnected porous web network. The uneven porosity was observed in the whole picture. Such type of morphology may be observed due to ignition at the end of reaction. This morphology could be shows good agreement for surface chemical reactions because it provides greater surface area and such conditions are favorable for the sensing mechanism.

Energy dispersive X-Ray analysis (EDAX) data in Fig 3 shows a sharp peak of ZnO without any impurity. Compositional percentage of chemically synthesized ZnO samples by Combustion methods is also found correct. It clearly indicates that samples of Zn had been successfully synthesized by chemical combustion method. The composition values shows the weight % and atomic % of Zn and O. The total % of Zn and O is 100 so it indicates that no any other impurity was found in synthesized ZnO nanoparticles.

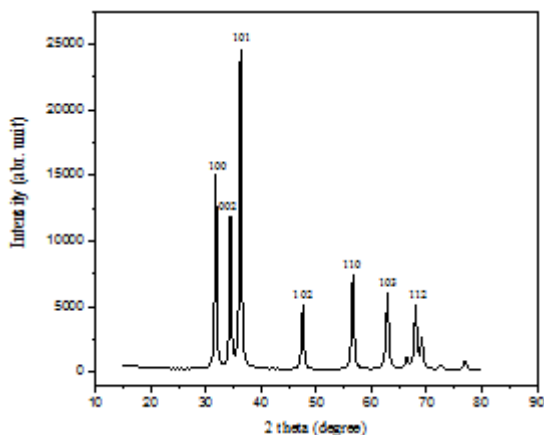


Figure 1: X-Ray Diffraction pattern of ZnO sample

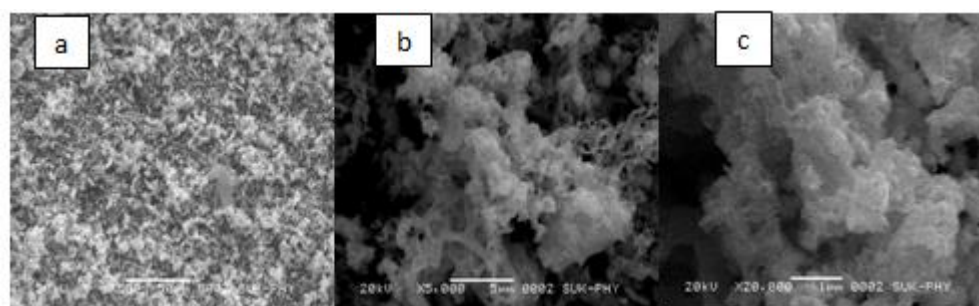


Figure 2: SEM images of ZnO (a),(b),(c) with magnifications of 50, 5 and 1 μ m respectively

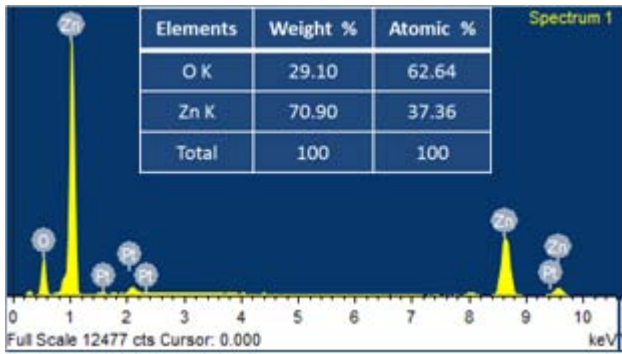


Figure 3: EDAX of ZnO and its elemental composition

3.4 UV-Visible Spectroscopy Study

The optical absorbance was recorded in the wavelength range of 200–900 nm. Zinc oxide is a direct band gap material and the energy gap (E_g) can thus be estimated by assuming direct transition between conduction band and valance bands. Theory of optical absorption gives the relationship between the absorption coefficients α and the photon energy ($h\nu$) as,

$$(\alpha h\nu)^2 = A (h\nu - E_g)^{n/2} \dots\dots\dots(2)$$

Where, A is the function of index of refraction and hole/electron effective masses [25] and α is the optical absorbance and 'n' is a number equal to 4 for direct band gap and 1 for the indirect band gap semiconductors. Figure 4 shows the Plot of $(\alpha h\nu)^2$ against $h\nu$. The observed value of E_g for ZnO is 3.2eV.

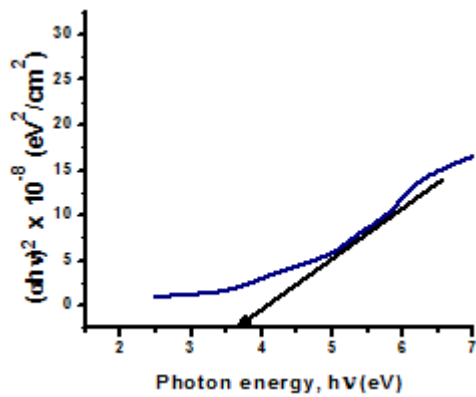


Figure 4: Graph of $(h\nu)$ versus $(\alpha h\nu)^2$ of ZnO

3.5 Electrical Resistivity Measurement

In the present study, the electrical resistivity of ZnO films was measured by conventional d. c. two-probe method in the range of 300 to 600 K. A chromel-alumel thermocouple (24 gauge) was used to measure the temperature. The silver paste contacts of 1 mm separated by 1 cm were used to form Ohmic contacts.

Initially, the nature of electrical contact and film was measured within ± 10 V and it was found that in the above voltage range, the electrical contacts showed the ohmic behavior. Fig.5 shows resistance variation of the films with temperature in air atmosphere. There is decrease in resistance with increase in temperature indicating semiconducting behavior obeying $R = R_0 e^{-\Delta E/kT}$ in the temperature range 300 K to 600 K.

Activation energy of ZnO film was calculated from Arrhenius plot for low and high temperature regions. Fig.6 shows $\log \rho$ versus reciprocal of temperature ($1000/T$) variation of the different samples.

$$R = R_0 e^{-\Delta E/kT}$$

Where, R_0 = Resistance at constant temperature, ΔE = the activation energy of the electron transport in the conduction band, The room temperature resistivity of ZnO was found to be $6.422 \times 10^3 \Omega\text{-cm}$. The activation energy in the lower temperature region is 0.19eV while it is 0.42eV in the higher temperature region

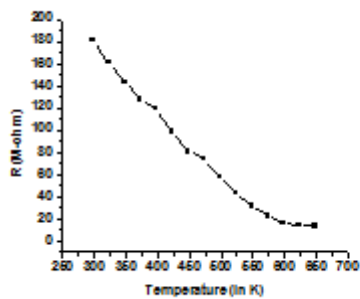


Figure 5

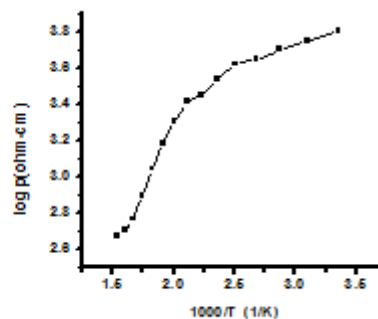


Figure 6

Fig.5 Variation of resistance Vs temperature for ZnO

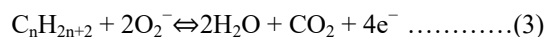
Fig.6 Electrical resistivity of the films onto glass substrate with reciprocal of temp ($1000/T$)

3.6 Gas Response Characteristic

Mechanism for the gas sensing of n-type semiconducting metal oxide is based on the electron transport between the sensor surface and chemisorbed species that modify the

surface conductivity of the sensor [26]. When the sensor is exposed to air, the atmospheric oxygen species are adsorbed on the surface of sensor, and then capture electrons from the conduction band to form the chemisorbed oxygen species (O_2^- , O^- , O^{2-}) depending on sensor temperature. Gas sensitivity of synthesized ZnO was recorded in the form of change in resistance on digital multimeter in the range of Mega Ohm. followed by using the sensitivity formula [27-28]. As the temperature strongly affects on sensor performance, we systematically investigated effect of temperature on sensing performance of ZnO film at the interval of 25^oC. Fig 5 clearly shows that gas response increases accordingly with respect to temperature. At temperature 300^oC highest gas sensitivity (S=54%) was observed and It again decreases at temperature 325^oC. So for further analysis 300^oC optimum gas operating temperature was fixed.

smaller concentration of gas, lower sensitivity is observed due to lower surface coverage of gas molecules. An increase in the gas concentration raises the surface reaction due to larger surface coverage. A further increase in surface reaction will be stable when the saturation point of the coverage of molecules is reached. It is well recognized that LPG consists of CH₄, C₃H₈, C₄H₁₀, etc., and in these molecules the reducing hydrogen species are attached to carbon atoms. When the nano-sized ZnO is exposed to reducing gas like LPG, the LPG responds with the chemisorbed oxygen and thus releasing an electron back to the conduction band which decreases the resistance of the ZnO. The overall reaction of LPG molecules with adsorbed oxygen can be shown in equation (3) for n=1. Subsequently methane reacts with this adsorbed oxygen and produces H₂O and CO₂. [29-30]



It is evident from Fig 6 that as the LPG gas concentration increases sensitivity of ZnO sensor also increases. For a

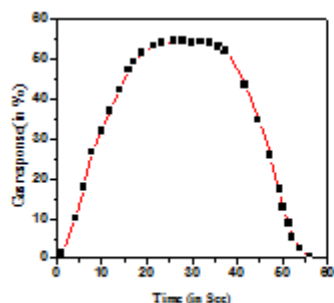


Figure 7

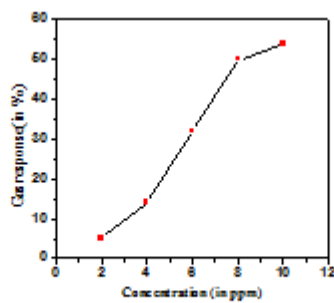


Figure 8

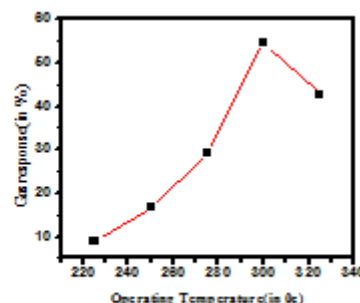


Figure 9

Fig 7: Dynamic sensing transient of ammonia gas at different operating temperature

Fig 8: Dynamic sensing transient of gas response at different time.

Fig 9: Dynamic sensing transient for ZnO at different ammonia gas concentration at temp. 300^oC

Optical study shows that band gap 3.2 eV. was observed. 43% highest ammonia gas sensing response was recorded at temperature 300^oC for 100 ppm ammonia gas concentration. Effect of gas concentration study shows that gas sensitivity (S%) increases gradually with increase in gas concentration.

5. Acknowledgement

Author is gratefully thankful to University Grant Commission, New Delhi for sanctioning financial assistance under the scheme of minor research project.

References

- [1] RYU H., PARK B., AKBAR S. A., *Sensor and actuators B*, 151(1) (2010), 107-113.
- [2] TAN T.L., LAI C. W., BEE S. HAMID A. *Hindavi publishing corporation*, (2014).
- [3] HAO Y., LOU S., ZHOU S. YUAN R., *nanscale research. Letters*, 7(1) (2012), 100.
- [4] DUC N., VAN QUANG V., KIM D., *J. Alloys compd*, 549 (2013), 260-268.
- [5] BALOURIA V., SAMANTA S., *Sensor and actuators B Chem*. 176 (2013), 1-26.
- [6] BAUER M., WEIMER U., SIMON I., BA N., *Sensors and actuators B*, 73 (2001), 1-26.
- [7] AN W., *Research on precision instrument and machinery*, 1(1) (2012), 1-5.

Table 1: summary of ZnO gas sensor for LPG gas

Synthesis Method	Operating temp (K)	Gas concentration	Sensitivity	References
SILAR	300	1.6vol %	75%	[31]
CBD	523	1.6 Vol.%	88%	[32]
Hydrothermal	523	5000 ppm	15.3	[33]
Hydrothermal	423	100 ppp	20	[34]
Spray Pyrolysis	673	0.4 Vol. %	43%	[35]
SILAR	673	0.4 Vol. %	28%	[36]
CBD	673	0.2 Vol.%	28%	[37]
Wet Chemical	548	200 ppm	2700	[38]
CBD	673	0.2 Vol.%	75%	[39]
Ultrasonication	573	1000 ppm	1727	[40]
Mechanochemical	R.T.	4 vol. %	12.3	[41]
Combustion	573	10 ppm	54.3	[Present Work]

4. Conclusion

ZnO nanoparticles have been synthesized successfully by combustion method. Structural property shows hexagonal wurtzite crystal structure with particle size 22.77 nm. Morphology was observed with high porous cavity. The

- [8] BAI Z., XIE C., ZHANG S., *Sensor and actuators Bchem.* 151(1) (2010), 107-113.
- [9] ANNISH P. M., VANAJA K.A., *nanophotonic material IV* 6639 (2007), 1-9.
- [10] HJIRI M., EI MIR L., LEONARDI S. G., *Nanomaterials*, 2 (2013), 357-369.
- [11] SHINDE V. R., LOKHANDE C. D., *Applied surface science*, 245 (2005), 407-413.
- [12] SARMA H., CHAKRABORTTY D., SARMA K., 3(10) (2014), 16957-16964.
- [13] SHINDE V., GUJAR T., *Materials chemistry and physics*, 120 (2007), 551-559.
- [14] A. S. C., HONGSITH N., MANGKOMTONG P., *Physica E*, (2007) 10-13.
- [15] RONNING C., GAO P. X., DING Y., *Applied physics letters*, 84(5) (2004), 783-785.
- [16] WANG X. ZHANG Z., ZHOU F., *Applied surface science*, 252 (2006), 2404-2411.
- [17] MA Y., ZHANG Z., ZHOU F., LU L., JIN A., *Nanotechnology*, 16(6) (2005), 746-749.
- [18] DHAS V., MUDHULI S., LEE W., *Applied physics letters*, 93 (2008), 312408.
- [19] YI S., CHOI S., JANG J., KIM J., *J. colloid and surface science* 313(3) (2007) 705-710.
- [20] LOOK D.C., *Semicond.Sci. Technol*, 20 (2005), 55-61
- [21] MOTE V.D., DHOLE B.N., *Universal J. of physics and applications*, 2(1)(2014), 10-13
- [22] MURUGESAN N., ACHUTHANUNNI A., *Suranaree J. sci. technol.* 18(1) (2011) 81-88
- [23] SHINDE V.R., GUJAR T.P., LOKHANDE C.D., *Sensors and actuators B*, (2006)
- [24] BIE L., YAN X., YIN J., DUAN Y., *Sensors and actuators*, 126 (2007) 604-608.
- [25] A. KAJBAFVALA, R. SHAYEGH M, *J. Alloys and compounds*, 469 (2009) 293-297.
- [26] B. Mondal, B. Basumatari, J. Das, *Sens. Actuators, B: Chem.* 194 (2014) 389.
- [27] WANG C., YIN L., ZHANG L., GAO R. *Sensors* 2088-2106 (2010).
- [28] BASU P. K. BHATTACHARYA P., *Sensors and actuators B*, 133 (2008) 357-363.
- [29] V.R. Shinde, T.P. Gujar, C.D. Lokhande, *Sens. Actuators B* 120 (2007) 551.
- [30] BASU P.K., JANA S.K., SAHA H, *sensors and actuators B*, 135 (2008), 81-88.
- [31] P. Mitra, A. P. Chatterjee, and H. S. Maiti, *Mater. Lett.* 35 (1998) 33.
- [32] P. Mitra and H. S. Maiti, *Sens. Actuators B* 97 (2004) 49.
- [33] X. Jiaqiang, C. Yuping, C. Yadong and S. Jianian, *J. Mater. Sci.*, 40 (2005).
- [34] B. Baruwati, D. K. Kumar, and S. V. Manorama, *Sens. Actuators B* 119, (2006) 676.
- [35] V. R. Shinde, T. P. Gujar, and C. D. Lokhande, *Sens. Actuators B* 120, (2007) 551.
- [36] V. R. Shinde, T. P. Gujar, C. D. Lokhande, *Sens. Actuators B* 123 (2007) 882.
- [37] V. R. Shinde, T. P. Gujar, C. D. Lokhande, *Mater. Sci. Eng. B* 1 (2007) 119.
- [38] S. C. Navale, S. W. Gosavi and I. S. Mulla, *Talanta* (2008) "Accepted manuscript".
- [39] C.D. Lokhande, P.M. Gondkara, *J. of Alloys and Compounds* 475 (2009) 304-11
- [40] L.A Patil, A. R. Bari, M.D. Shinde, *Sens. and Actuators B* 149(1) (2010) 79-86.